Modelling the Hydrodynamics of an L-shaped Breakwater

S Pan[1], N MacDonald[2], P Sayers[3], J Nicholson[1] & B A O'Connor[1]
[1]*Department of Civil Engineering, The University of Liverpool Brownlow Street, Liverpool, UK, L69 3BX, <S.Pan@liv.ac.uk>*
[2]*Canadian Hydraulics Centre, National Research Council, Montreal Road, Ottawa, Ontario, Canada, K1A 0R6 <Neil.MacDonald@nrc.ca>*
[3]*HR Wallingford Ltd, Howbery Park, Wallingford, Oxfordshire, UK, OX10 8BA, <pbs@hrwallingford.co.uk>*

Abstract

This paper describes physical and numerical modelling of the hydrodynamics associated with an L-shaped breakwater. The physical modelling was carried out using the UK Coastal Research Facility (UKCRF) at HR Wallingford as a part of a UK government EPSRC (Engineering and Physical Science Research Council) funded research project. An L-shaped breakwater was built on a plain bed with 1:20 bed slope. Normal and oblique monochromatic (MON) and long-crested random (LCR) incident waves were employed in the tests. Measurements of waves and currents were taken around the breakwater. A 2D wave period-averaged wave/current model was applied to the laboratory situations. The numerical model allowed for wave diffraction-refraction and wave/current interaction to be considered. Comparisons of the numerical model results with the experimental data were made and good agreement in both the wave-induced currents and wave heights was obtained. The results demonstrated the capability of the model in dealing with hydrodynamics over a complex bathymetry, in particular, the hydrodynamics associated with wide-angle diffraction.

1 Introduction

L-shaped breakwaters have been commonly used to protect harbours and beaches from wave attack. However, the design of these coastal structures and the prediction of morphodynamic change caused by these structures

require a deep understanding of the relevant hydrodynamics. Numerical models have increasingly been used as a powerful tool to solve some of these problems, but not all. Physical models are still needed to achieve a better understanding the detailed physical features of the hydrodynamics, as well as to provide valuable data sets for numerical model validations. As a result, the UKCRF, co-sponsored by the EPSRC and HR Wallingford, has provided a well-controlled experimental environment in which physical modelling involving the wave, current and coastal structure interactions can be conducted. Details of the UKCRF can be found elsewhere (see Simon et al, 1995).

A series of physical model tests has been carried out by researchers from the Maritime Coastal Group at Liverpool University led by Professor O'Connor, in collaboration with researchers from other two UK universities, namely Imperial College led by Dr Anastasiou and University College London led by Dr Simons. One of these test series investigated the hydrodynamics associated with an L-shaped breakwater, details of which are described in this paper. The experimental results are then compared with the results obtained from a wave/current numerical model, details of which are also described in this paper.

2 Experiment Layout

The UKCRF provides a test area of 36 m in the longshore direction by approximately 22 m in the cross-shore direction. Waves are generated by 72 paddles using the HR WAVEGEN software, which is capable of creating normal and oblique (up to 30 degrees to the shore normal) monochromatic and long/short-crested random seas. It is also possible to superimpose a longshore current through four sets of pumps located in sumps at both ends of the basin. A particular longshore current profile can be achieved by adjusting 40 undershot sluice gates at each end and the flow rate assigned to each pump. Wave and current measurements can be taken at any point in the central area of the basin by mounting instruments on a programmable 3D positioner, known as *the bridge*.

In this particular physical model, an L-shaped breakwater, measuring 6 m by 6 m, was constructed on a 1:20 sloping bed. The water depth at the wave paddles was set to 0.5 m. The layout of the experiment is illustrated in Figure 1. The L-shaped breakwater was situated in the central area of the basin using 12 mm plywood sections to form an impermeable membrane defining the breakwater perimeter. Where exposed to direct

wave action the plywood was protected with wave energy-absorbing polyurethane foam. The thickness of the foam protection was adjusted to yield a transmission length through the foam of at least 50% of the local wave length so that it was sufficient to reduce reflection without being of an over-intrusive width. Prior to the foam material being used in the UKCRF, tests were carried out in a wave flume in Imperial College London revealed a wave reflection coefficient of less than 5%.

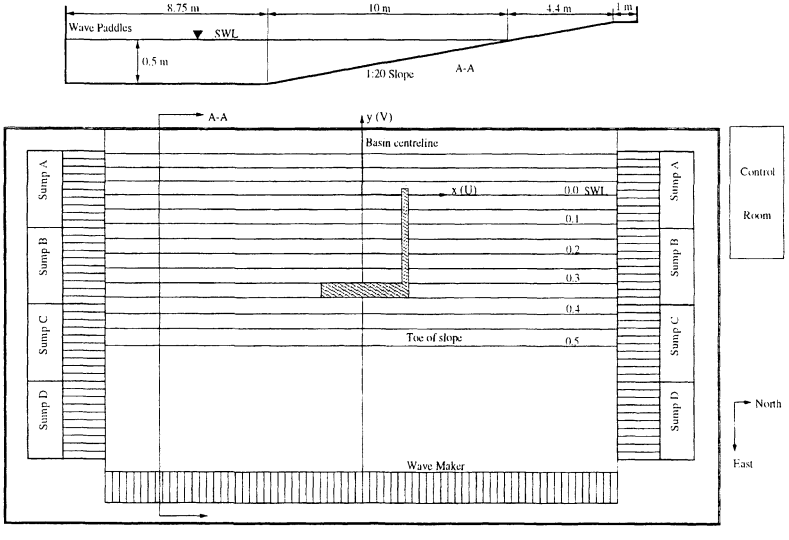

Figure 1 The UKCRF layout and position of the L-shaped breakwater

Offshore wave measurements were taken by resistance-type wave gauges at fixed positions on the outer boundary. Inshore waves and currents were measured at various positions by a nearshore wave gauge and an Ultrasonic Current Meter (UCM) mounted on the bridge. These positions are shown in Figure 2. All data were logged using the Dplus data acquisition system for future analysis. The recording length was taken as 100 waves for monochromatic waves and 500 waves for random waves (see Sayers et al, 1995 for details related to the data acquisition and data analysis).

Although it was possible to superimpose a longshore current through the sumps at both ends as mentioned previously, no longshore current was superimposed in order to keep the experimental conditions as simple as possible.

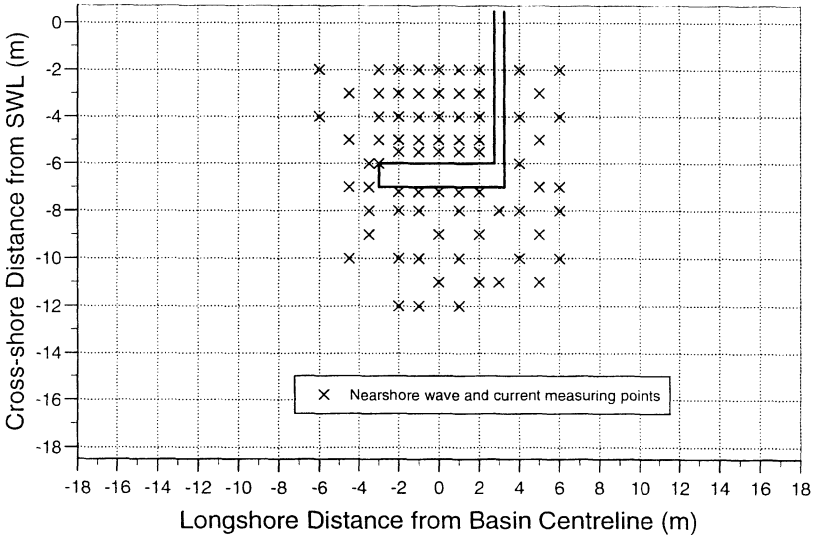

Figure 2 Locations of nearshore wave and current measurements

3 Test Conditions

Experiments with three sea states were performed using the same breakwater configuration outlined previously. Details of these test conditions are listed in Table 1.

Table 1 Test conditions for the L-shaped breakwater

Test No	Wave Type	Target Wave Height (m)	Measured Wave Height (m)	Wave Period (sec)	Wave Direction (deg)
BW1	MON	0.10	0.082	1.0	0
BW2	MON	0.10	0.110	1.0	20
BW3	LCR	0.10	0.088	1.0	20

It should be noted that the values in the column "Measured Wave Height" in Table 1 were measurements taken 5 m from the wave paddles. The wave direction was measured anti-clockwise from shore-normal. In this paper, only the results obtained from Test No BW2 (oblique monochromatic incident waves), will be presented and discussed.

4 Numerical Model

A 2D wave period-averaged wave/current numerical model was applied to the laboratory situations and the wave field and wave-induced hydrodynamics were computed. The numerical model allowed wave diffraction-refraction and wave-current interactions to be considered. A two-equation turbulence model was also included to take account of the turbulence kinetic energy and energy dissipation rate distributions due to bed friction and wave breaking. The model, see Yoo & O'Connor (1986) and O'Connor & Yoo (1987), has been improved using data from the UKCRF to allow for interactive bed friction, random waves and wide-angle diffraction by structures (see MacDonald, 1998).

4.1 Governing Equations

The governing equations for wave motion were derived based on the assumptions that the system can be adequately described by linear small amplitude wave theory and as a 2D depth-averaged one, and the spatial variations of bottom bathymetry and current velocity are small compared to the wave length, as well as wave reflections are negligible. Therefore, the wave number vector and wave energy equations can be expressed as:

$$\frac{\partial K_i}{\partial t}+\left[C_g\frac{K_j}{k}+U_j\right]\frac{\partial K_i}{\partial x_j}+\frac{\sigma G}{2d}\frac{\partial d}{\partial x_i}+\frac{C_g}{2kA}\frac{\partial}{\partial x_i}\left[\frac{1}{A}\frac{\partial^2 A}{\partial x_j \partial x_j}\right]+K_j\frac{\partial U_i}{\partial x_j}=0 \qquad (1)$$

$$\frac{\partial A}{\partial t}+\frac{1}{2A}\frac{\partial}{\partial x_i}\left[A^2\left(\frac{C_g}{k}K_i+U_i\right)\right]+\frac{S_{ij}}{\rho g A}\frac{\partial U_j}{\partial x_i}+C^a A^2=0 \qquad (2)$$

where K_i = wave number vector (i =1, 2); U_i = current velocity (i=1, 2); A = wave amplitude; σ = intrinsic wave frequency, σ^2 = gk tanh(kd); C_g = wave group velocity; G = 2kd/sinh(2kd); C^a = wave energy dissipation coefficient due to wave and current shear stresses and wave breaking; k = wave separation factor; x_i = co-ordinate (i = 1, 2); t = time and d = water depth.

The governing equations for depth-averaged wave-induced currents are the continuity and momentum equations expressed as follows:

$$\frac{\partial \eta}{\partial t}+\frac{\partial}{\partial x_i}(dU_i)=0 \tag{3}$$

$$\frac{\partial U_i}{\partial t}+U_j\frac{\partial U_i}{\partial x_j}+\frac{1}{\rho d}\frac{\partial S_{ij}}{\partial x_j}+g\frac{\partial \eta}{\partial x_i}+\frac{(U_jU_j)^{1/2}}{d}C_vU_i-\frac{\partial}{\partial x_j}\left(\nu\frac{\partial U_i}{\partial x_j}\right)=0 \tag{4}$$

where η = surface elevation; S_{ij} = radiation stress; C_v = friction factor due to a current and ν = eddy viscosity, which can be calculated using turbulence kinetic energy and energy dissipation equations as follows:

$$\nu=M\kappa^{1/2}\min\left(C_D\frac{\kappa^{1/2}}{\epsilon},2A\right) \tag{5}$$

$$\frac{\partial \kappa}{\partial t}+U_j\frac{\partial \kappa}{\partial x_j}-\frac{\partial}{\partial x_j}\left(\frac{\nu}{\Gamma_\kappa}\frac{\partial \kappa}{\partial x_j}\right)-P_\kappa+\epsilon=0 \tag{6}$$

$$\frac{\partial \epsilon}{\partial t}+U_j\frac{\partial \epsilon}{\partial x_j}-\frac{\partial}{\partial x_j}\left(\frac{\nu}{\Gamma_\epsilon}\frac{\partial \epsilon}{\partial x_j}\right)-P_\epsilon+C_2\frac{\epsilon^2}{\kappa}=0 \tag{7}$$

$$P_\kappa=\frac{1}{\rho d}(D_{BF}+D_{WF}+D_{CF}) \tag{8}$$

$$P_\epsilon=\frac{1}{4}C_2\left(C_D\frac{\kappa}{A}\right) \tag{9}$$

where M = 0.4; C_D = 0.225; C_2 = 1.92; Γ_κ = 1.0; Γ_ε = 1.3; $D_{WF} = \rho C_w U_o^3$; $D_{CF} = \rho C_v U^3$; C_w = friction factor due to waves; U_o = maximum orbital velocity; U = resultant current velocity; D_{BF} = energy dissipation due to wave breaking which is described later.

4.2 Wave Breaking Criterion

In the present work, a simple wave breaking criterion was used so that a wave was considered to have broken when the ratio of the wave height to the local water depth exceeded a certain value (0.79 in this paper). This criterion was used to determine the wave breaking line or the first breaking point. Waves were also regarded as broken at any shoreward points if the wave had broken at any "upwind" points based on the local

wave direction.

If the wave at any point had been marked as broken, an amount of wave energy was then subtracted from the wave energy equation (Eq. 2) as a sink term equivalent to the energy loss in a hydraulic jump. The following expression was used (Fredsøe & Deigaard, 1992):

$$D_{BF} = \frac{2\rho g A^3}{Td\left[1-\left(\frac{A}{d}\right)^2\right]} \tag{10}$$

The above equation can then be written in conjunction with the wave energy equation (Eq. 2) in the following form:

$$C^a = \frac{2}{Td}\frac{1}{\left[1-\beta^2\right]} \tag{11}$$

where T = wave period; β = A/d.

4.3 Numerical Scheme and Boundary Conditions

A finite difference method was used to discretise the governing equations. The computations were carried out with a staggered grid system, where the velocity and wave vectors are computed on the faces of a cell and scalar variables were computed in the centre of the cell (see MacDonald, 1998 for details). An up-wind scheme was also used for all convection terms in the governing equations and the equations were solved using a fully implicit method.

The wave boundary conditions were given at the wave paddles and closed boundary conditions were used at the north side of the basin to reflect the shadow area caused by the obliquely-incident waves. Absorbing boundary conditions were used at the south side to represent wave transmission and at the breakwater faces exposed to the incident waves to simulate the non-reflective boundaries. The shoreline was treated automatically in the section of the program dealing with dry/wet boundaries due to the flooding caused by the water surface setup.

5 Results

The computational domain covered the entire experimental area, which was divided into 73 x 47 grid points with a 0.5 m grid size in both the longshore and cross-shore directions. The computational time interval (dt)

was set to 0.05 seconds and the model was run for 100,000 time steps. The time series at selected positions were examined. The results showed that the wave and currents had reached a steady state at the end of the run. As the main interest was focused on the nearshore side of the L-shaped breakwater, the computed and measured results in this area are considered in the following discussions.

Figure 3 shows the computed velocity vectors compared with the measured results. It is clear that good agreement was obtained in terms of both velocity magnitude and direction. The current circulation was also reproduced well by the model as the centre of the gyre coincides with the measurements.

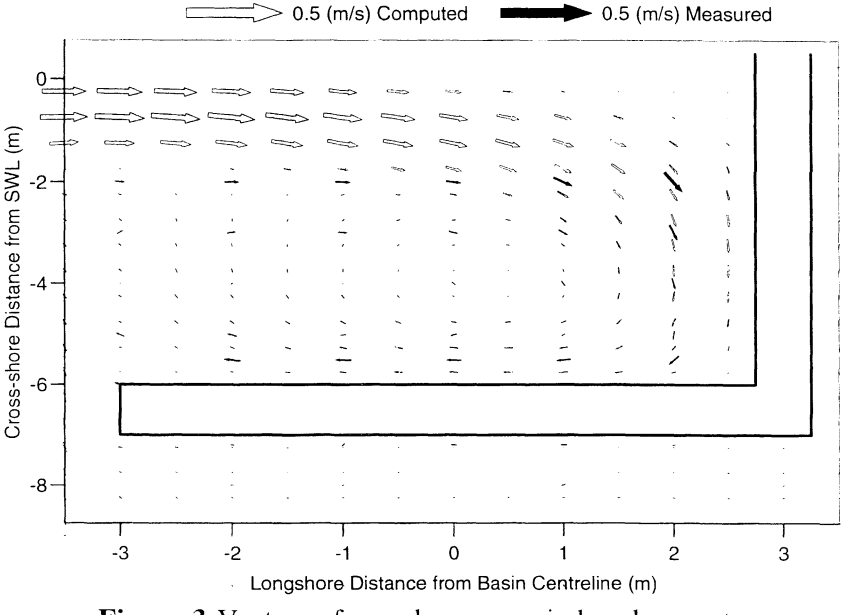

Figure 3 Vectors of nearshore wave-induced currents

Figure 4 shows the computed wave vectors, the length of each vector representing the wave height; the dots are the dry land and the co-ordinates are the computational grids. The wave diffraction due to the breakwater can be clearly seen. The wave direction remained at its incident value (20° anti-clockwise from the shore-normal) seawards of the breakwater and then waves were diffracted into the area behind the breakwater by the structure. In addition, both the numerical model and the experimental results showed a wave height increase in the area adjacent to the cross-shore wing (right-hand side) of the breakwater. For clarity,

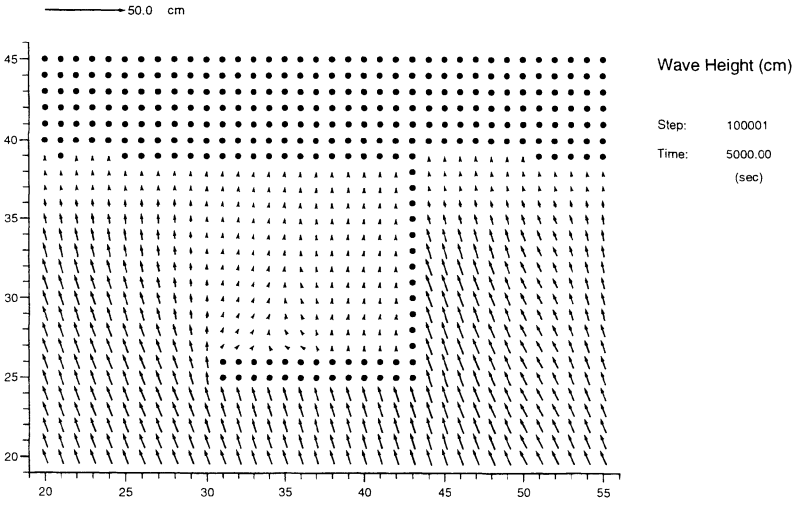

Figure 4 Wave height vectors

comparisons between the computed and measured wave heights were made along selected transects in both the longshore and cross-shore directions. Figures 5 and 6 show the comparisons of computed and measured wave heights along longshore sections y=-2, -4, -5 and -6 m from the still water line (SWL) (see Figure 2 for the positions). Good agreement was obtained for all these transects. In addition, Figure 7 shows a similar comparison along cross-shore sections x=-2 and -3 m from the basin centreline. Since the wave heights inside the L-shaped breakwater are generally small, the computed wave heights agree reasonably closely with the measured values.

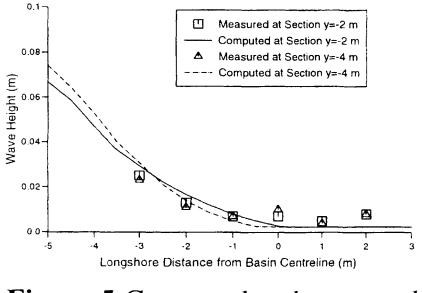

Figure 5 Computed and measured wave heights along longshore sections (y=-2 and -4 m from SWL)

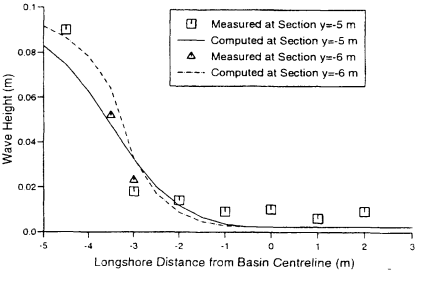

Figure 6 Computed and measured wave heights along longshore sections (y=-5 and -6 m from SWL)

6 Conclusions

A physical model and a numerical model have been described. The numerical model was applied to an hydraulic model test associated with an L-shaped breakwater. The comparison between the computed and measured results showed good agreement for both wave heights and wave-induced currents. These results indicated that the physical model provided valuable data sets for numerical model validations and that the numerical model was capable of dealing with wide-angle diffraction caused by the L-shaped breakwater.

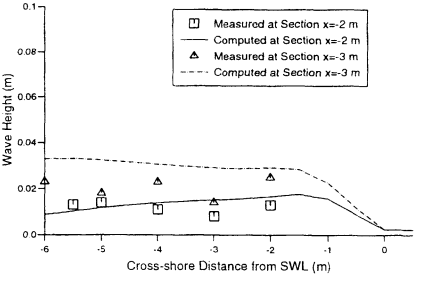

Figure 7 Computed and measured wave heights along cross-shore sections (x=-2 and -3 m from the basin centreline)

Acknowledgements

The work was financially supported by EPSRC, HR Wallingford and the Commission of the European Communities Directorate General for Science and Education, Research and Development under contract numbers GR/J25017, GR/K48600, MAS3-CT97-0086 and MAS3-CT97-0106. The authors would like to express their gratitude for the assistance provided by Y. Zhao of Imperial College and R. MacIver of University College London and also by A. Channell, the UKCRF Operator, and R. Whitehouse, the former UKCRF Manager during the course of the experiment.

References

Fredsøe, J. and Deigaard, R., (1992), Mechanics of coastal sediment transport, World Scientific, Singapore

MacDonald, N. J., (1998), Numerical modelling of non-linear wave-induced nearshore circulation, PhD thesis, Dept. of Civil Engineering, The University of Liverpool

O'Connor, B. A. and Yoo, D., (1987), Turbulence modelling of surf zone mixing processes, Proc. Coastal Hydrodynamics Conf., ASCE, pp 371-383

Sayers, P. B., O'Connor, B. A. and MacDonald, N. J., (1995), Wave-current interaction in random waves and currents - Physical model testing in the UKCRF, Dept. of Civil Engineering, The University of Liverpool, Report No. CE/10/95

Simons, R., Whitehouse, R., MacIver, R., Pearson, J., Sayers, P., Zhao, Y. and Channell, A. (1995), Evaluation of the UK Coastal Research Facility, *Coastal Dynamics '95*, Dally, W.R. and Zeidler, R.B. (eds), ASCE, New York, pp 161-172

Yoo, D. and O'Connor, B. A., (1986), Mathematical modelling of wave-induced nearshore circulations, Proc. 20th ICCE, ASCE, 3, pp 1667-1681